*Valeeprakhon & Eua-Anant, 2015*

*Volume 1 Issue 1, pp. 132-143*

*Year of Publication: 2015*

*DOI- https://dx.doi.org/10.20319/mijst.2016.s11.132143*

*This paper can be cited as: Valeeprakhon, T., & Eua-Anant, N. (2015). Segmentation of Connected Red Blood Cells Based on Distance per Displacement Ratio Maximization Criterion. MATTER: International Journal of Science and Technology, 1(1), 132-143.*



# SEGMENTATION OF CONNECTED RED BLOOD CELLS BASED ON DISTANCE PER DISPLACEMENT RATIO MAXIMIZATION CRITERION

**Tamnuwat Valeeprakhon**
*Department of Computer Engineering, Faculty of Engineering, Khon Kaen University, Khon Kaen, Thailand*
*tamnuwatv@kkumail.com*

**Nawapak Eua-Anant**
*Department of Computer Engineering, Faculty of Engineering, Khon Kaen University, Khon Kaen, Thailand*
*nawapak@kku.ac.th*

---

## Abstract

*Red blood cell counting is difficult to perform by automated visual inspection because of the large number of connected RBCs in blood smear slides. This paper presents anew algorithm to segment connected RBCs in blood smear images based on the distance per displacement ratio criterion. First, RBCs were separated from white blood cells and platelets by performing thresholding on the b* component in Lab color space. Next, connected RBCs and single RBCs were separated by using the Circular Compactness Shape Factor criterion. Later, points on boundaries of connected RBCs with high curvature were marked as concave points. Each concave point was then paired to a nearby concave point that maximizes the distance per displacement ratio criterion. Finally, a set of paired concave points was used as information for segmenting connected RBCs. Experimental results of RBC counting, including connected and single RBCs, on 50 blood smear images, revealed that the*

*proposed algorithm can achieve an average accuracy of up to 99.22%.*

**Keywords**

Red Blood Cell Counting, Segmentation of Connected Red Blood Cells, Circular Compactness Shape Factor, the Distance per Displacement Ratio

## 1. Introduction

Blood diseases are one category of diseases that affect numerous patients, worldwide. In Southeast Asian countries, surveys of results from hospitals found that the ratio between the numbers of patients with blood diseases and other diseases was up to 47% (Kanitsap 2010). Such diseases can be diagnosed from blood tests to find infection, unusual shapes and unusual numbers of blood components, e.g., red blood cell (RBC), white blood cell (WBC), platelets and plasma (Kareem et al., 2011). Unusual numbers of cells can occur within any cell types, especially RBCs. In order to diagnose the unusual number of RBCs, counting methods were usually employed (Pradipta et al., 2015). RBC counting can be used as a part of a health checkup in order to verify for a diversity of conditions and help to diagnose and monitor a number of diseases that were identified by the production and lifespan of RBCs (Lorenzo et al., 2013). An unusual number of RBCs means that there are a higher or lower than the normal number of RBCs. The standard numbers of RBCs may vary slightly among different laboratories. For example, the standard numbers that most technicians use are 5.4-6.0 M/µl for males and 4.0-5.0 M/µl for females (Sumeet et al., 2014). Normally, a RBC is flexible, has oval biconcave disks and lacks a cell nucleus. A typical RBC has a disk diameter of approximately 6.2–8.2µm and a thickness at its thickest point of 2–2.5µm (Site et al., 2013). RBC counting using human visual inspection is difficult and quite a slow process because of the large number of RBCs in each blood smear image, many of them connected together (Pradipta et al., 2015).

In this paper, we present an algorithm that focuses on segmentation of connected RBCs in blood smear images in order to ease the RBC counting process as well as to improve RBC counting accuracy. The experimental results of RBC counting performed on 50 blood smear images are given.

## 2. Method

The overall process consists of 5 steps which are; preprocessing (noise removal), separation of RBCs from other blood components, discrimination between connected RBCs and single RBCs, segmentation of connected RBCs and RBC counting.

### 2.1 Preprocessing

In general, blood smears are stained using Giemsa or other stains and photographed using a microscope camera with 100X magnification. Generally, blood smear images not only contain blood components but also noise spread over the images (Heidi et al., 2011). A median filter is widely applied in the first step in order to remove noise and smooth the RBC images. An example of a median-filtered RBC image, using a window of size 5x5 pixels, is shown in Figure 1(A).

### 2.2 Separation of RBCs from other blood components

In the RBC counting procedure, only RBCs are of interest and hence must be separated from the other blood components, e.g., WBCs and platelets (Nasrul et al., 2013). Separation of RBCs from other blood components in a blood smear image is performed by thresholding the b* component in Lab color space. Normally, WBCs and platelets have lower yellow color components than RBCs (Lorenzo et al., 2013) and hence appear as dark areas in the b* component image as shown in Figure 1(B).Contrast stretching is then applied to increase contrast between WBCs and platelets and other components as shown in Figure 1(C). Next, a binary image containing only WBCs and platelets is obtained by thresholding the contrast enhanced b* image, using the Otsu method, followed by region filling as shown in Figure 2(A).

Furthermore, in order to extract the background of an image, the background is mostly brighter than the other objects and therefore can be extracted by converting a RGB blood smear image into a grey scale image, followed by thresholding using the Otsu method resulting in a background image as shown in Figure 2(B).

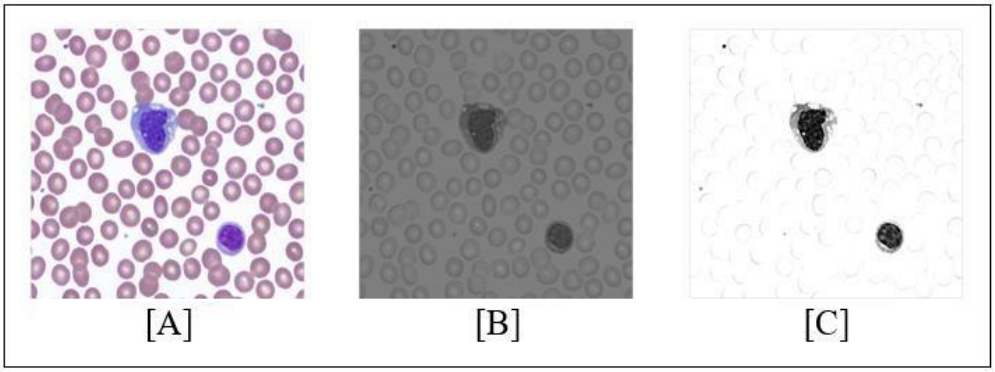


**Figure 1:** *(A) RGB blood smear image, (B) original b* component image, (C) b* component image after contrast stretching*.

Finally, an RBC binary image is extracted by subtracting the WBC binary image with the background image. This is followed by noise removal using a morphological opening operation with a disk-shaped structuring element with a radius of two pixels. The resultant RBC binary image is illustrated in Figure 2(C).

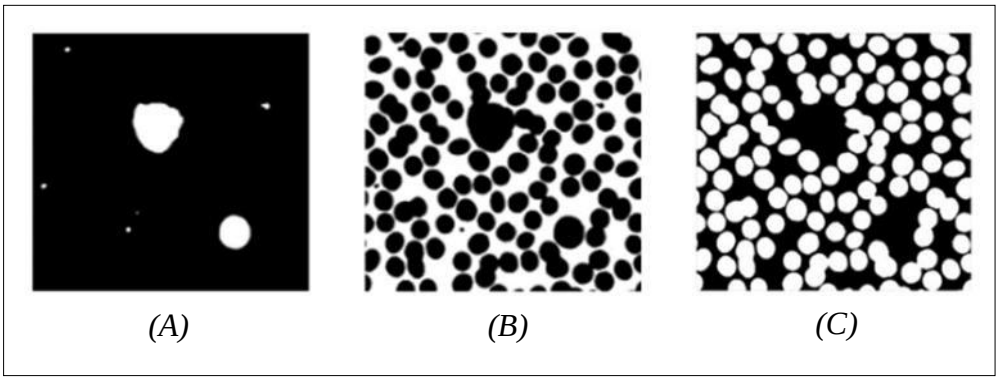


**Figure 2:** *(A) WBC binary image, (B) Background binary image and (C) RBC binary image.*

### 2.3 Discrimination between connected RBCs and single RBCs

After separating RBCs from other blood components, the next major step are to locate and segment connected RBCs. Without this step, connected RBCs can lead to inaccurate RBC counting. To order to discriminate connected RBCs from single RBCs, one promising feature that can accomplish this task is the circular compactness shape (CCS), a factor of a region defined as the ratio between region area $A(R)$ and the square of region perimeter $P^2(R)$ in Equation 1:

$$\mathrm{CCS} = 4\pi \frac{A(R)}{P^2(R)} \qquad (1)$$

Ideally, a perfect circular object yields the highest CCS factor of 1.0. Therefore single RBCs, with nearly circular shapes, will have a much higher CCS factor (around 1.0) than those of the elongated, connected RBCs. This is due to the fact that a region's perimeter increases linearly with the expansion factor while the region's area increases quadratic ally (Wilhelm et al., 2011).

To calculate the CCS factor of each region, the 4-connectivity connected-component labeling method is first exploited in order to label connected pixels of all regions. Then the region's area can be measured by counting pixels belonging to each region while the region perimeter is calculated by converting the region boundary contour into an 8-directional chain code and counting the chain code steps with vertical and horizontal segments (chain code = 0, 2,

4, 6) weighted by 1.0 and diagonal segments (chain code = 1, 3, 5, 7) weighted by as described in Equation 2:

$$P(R) = \sum_{i=1}^{M} Length(C_i) \quad (2)$$

Where

$$length(C) = \begin{cases} 1 & \text{for c} = 0,2,4,6 \\ \sqrt{2} & \text{for c} = 1,3,5,7 \end{cases}$$

Figure 3(A) illustrates examples of CCS factors of RBCs. As seen, single RBCs have a CCS factor around 1.0 while connected RBCs have lower CCS factors. Thus, by using a threshold value of 0.95, regions with CCS factors greater than 0.95 are taken into account as single RBCs while those with CCS factors lower than 0.95 are labeled as connected RBCs, as shown in Figure 3(B).

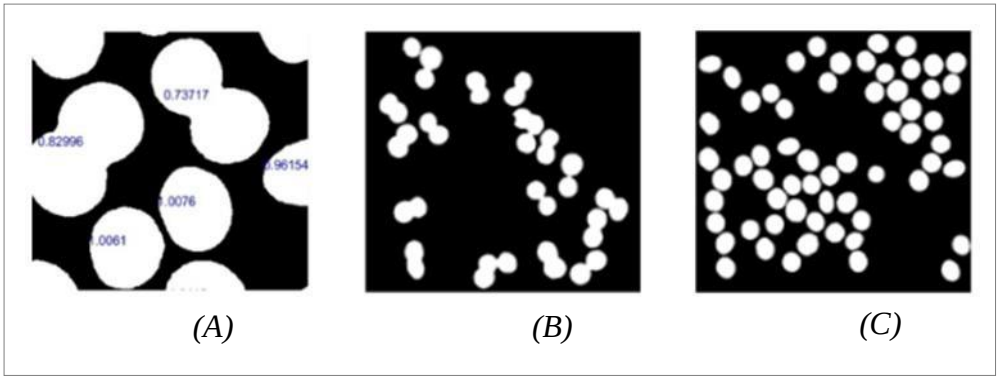


**Figure 3:** *(A) CCS factors of RBCs, (B) Connected RBCs, (C) Single RBCs.*

### 2.4 Segmentation of Connected RBCs

By nature, a normal RBC usually has a circular and convex shape (Siti et al., 2013), segmentation of connected RBCs can effectively be performed by exploiting the circular and convex figure of a normal RBC. In general, a convex object is defined as the smallest polygon that fits all points in the region (Wilhelm et al., 2011) and thus cannot contain concave points. On the other hand, connected RBCs are not convex but always have pairs of concave points between the boundaries of adjacent RBCs. Therefore, it is possible to separate connected RBCs from each other by pairing and cutting these concave points.

#### 2.4.1 Detection of Concave Points

Detection of concave points along the boundary of connected RBCs is an important step in segmenting connected RBCs accurately. A well-known feature for detecting concave points or corners is by curvature (Matt, 2013), for a 2-dimensional parametric curve, this is defined in Equation

3:

$$K = \frac{x'y'' - y'x''}{(x'^2 + y'^2)^{3}} \quad (3)$$

Normally, concave and convex points have high negative and positive curvature values, respectively, and therefore can be located by considering the curvature of each point along region boundaries. After obtaining a binary image of connected RBCs, a simple morphological boundary extraction algorithm is performed by subtracting the original binary image from an eroded binary image. Next, a sequence of boundary points $(x(t), y(t))$ of connected RBCs is extracted in a counter-clockwise direction as plotted in Figure 4(A).

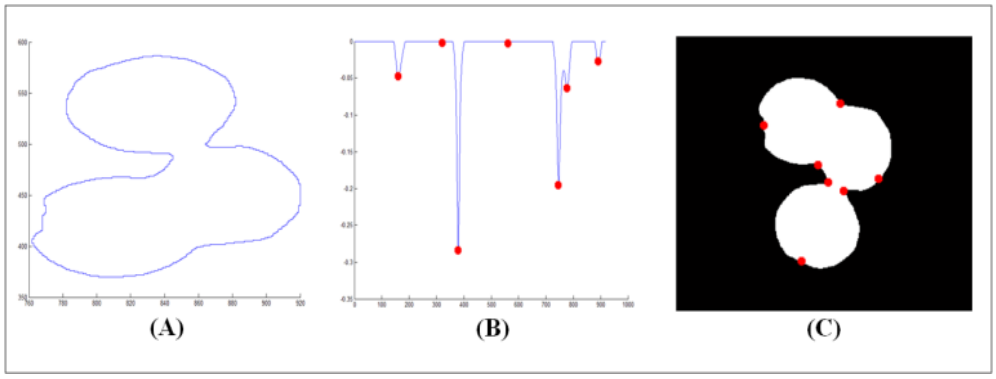


**Figure 4:** *(A) Boundary of connected RBCs, (B) Curvature graph and detected concave points, (C) Detected concave points.*

Derivatives $x'$, $x''$, $y'$ and $y''$ needed to calculate the curvature in Equation 4 are computed by using the frequency domain filtering technique. First, Discrete Fourier transforms of $x(t)$ and $y(t)$ is computed. In order to smooth jagged segments of the curves, a super-Gaussian low pass filter with a spread factor of 0.15 and filter power of 4is then applied. Finally, the $n^{th}$ derivative of a parametric curve is computed (Matt, 2013) using Equation 4:

$$x^{(n)}(t) = F^{-1}[(i\omega)^n X(i\omega)] \quad (4)$$

Where $X(i\omega) = F(x(t))$ is the discrete Fourier transform of $x(t)$.

After obtaining curvature values for all boundary points, only local maxima points with negative curvature values above the threshold value corresponding to concave points are selected, as shown in Figures 4(B) and 4(C)

### 2.4.2 Calculation of the Minimum Distance per Displacement Ratio

In order to segment connected RBCs accurately, concave points of connected RBCs must be paired correctly. A simple way to do this is to pair concave points using the nearest neighbor criterion. However, this method generally doesn't work when pairing isolated concave points or concave points of complicate objects.

In this paper, a new criterion based on maximizing the minimum distance per displacement ratio (MDDR) between concave points for segmenting connected convex objects, such as connected RBCs, is proposed. Here, distance is defined as the length of a path along a region boundary from a start point to an end point, while displacement is defined as the length of a straight line segment from the start point to the end point. For a given set of boundary points

$\{(x_0, y_0),(x_1, y_1),\square, (x_N, y_N)\}$ , distance (*Dt*) and displacement (*Dp*) are computed, respectively, using Equations 5 and 6 as in the following:

$$Dt = \sum_{i=0}^{N-1} \sqrt{(x_i - x_{i+1})^2 + (y_i - y_{i+1})^2} \quad (5)$$

$$Dp = (x_0 - x_N)^2 + (y_0 - y_N)^2 \quad (6)$$

For each pair of concave points in a close boundary, there are always 2 distance values, one measured in a clockwise direction ( $Dt_{cw}$ ) and another measured in a counter clockwise direction ( $Dt_{ccw}$) as shown in Figure 5. For segmentation task, only the minimum distance is of interest. The MDDR is hence given by

$$MDDR = \min(Dt_{cw}, Dt_{ccw}) / Dp \quad (7)$$

By finding a pair of concave points, among all possible pairs of concave points in a connected region, that maximizes the MDDR, then segmentation of connected convex objects can be achieved, object by object, repeatedly until all connected convex objects are separated. For the same displacement length, such a criterion guarantees that the rim connected RBC will most likely be the first object to be split.

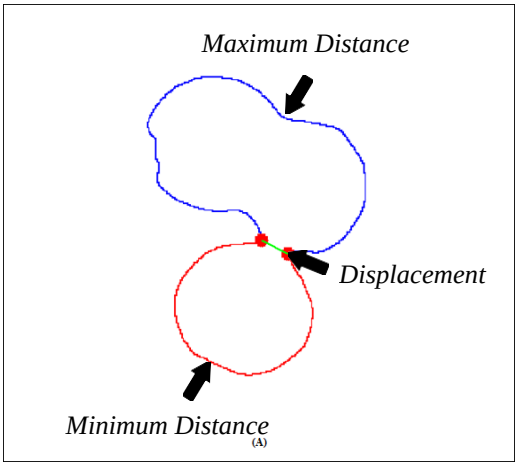


**Figure 5:** *Distances and displacement for computing the MDDR.*

### 2.4.3 Splitting connected RBCs

The proposed segmentation technique, based on maximizing the MDDR, as presented here can be applied to any connected convex objects. However, for precise segmentation of connected RBCs, in this paper, the proposed method can be applied along with this additional criterion: the area of each segmented, connected RBC must be lower than 1.2 times the maximum area of single RBCs. This condition is introduced in order to assure that the final segmentation result yields only single separated RBCs. If the area of the segmented region is higher than this value and there are unused concave points remaining in the segmented region, it is possible that there will still be more than one RBC existing in the segmented region. Thus, the segmentation process will be repeated until the areas of all segmented regions are lower than the threshold value.

### 2.5 RBC Counting

After achieving segmentation of connected RBCs, the final RBC counting task collects all information by counting all labeled single RBCs and split connected RBCs. Figure 6 shows the overall counting result of detected single RBCs and segmented connected RBCs.

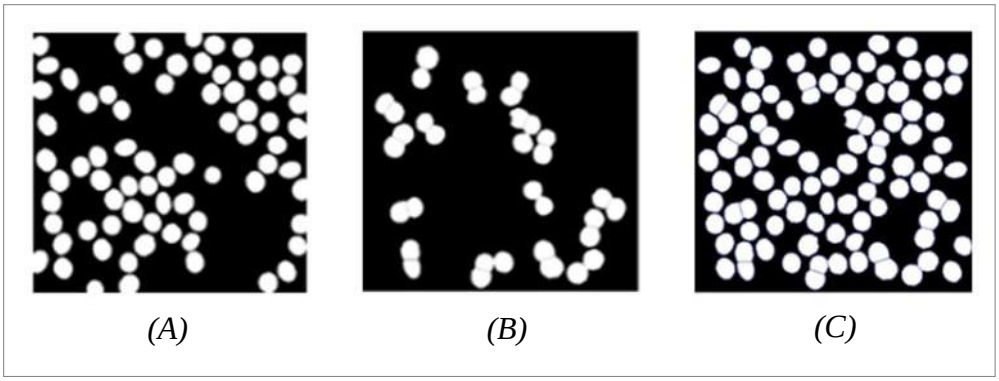


**Figure 6:** *(A) Single RBCs, (B) Split connected RBCs, (C) Overall results*

## 3. Results and Discussion

In this paper, 50 blood smear images were tested for RBC counting. Figure 7 demonstrates examples of tested blood smear images. It was found that the proposed method yields an overall counting result with average accuracy of 99.22% (95.98%-100%). The accuracy of each image is illustrated in Figure 7.

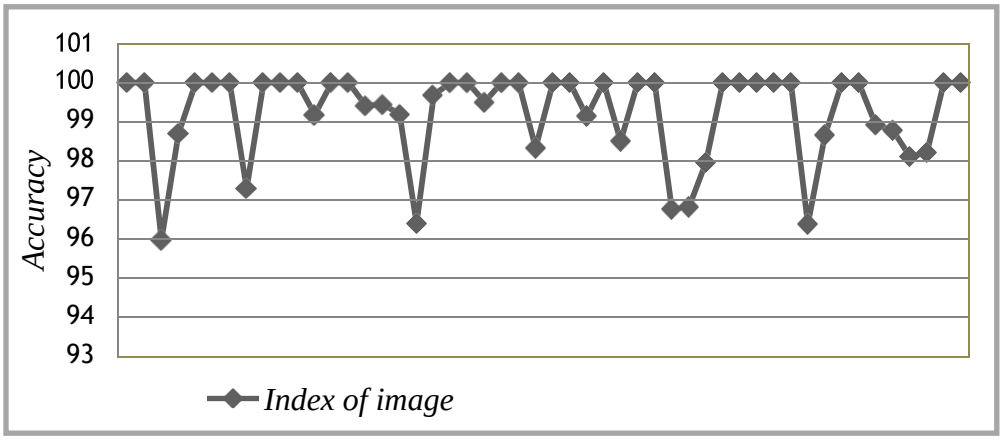


**Figure 7:** *Accuracy measure of each image*

In summary, the complete RBC counting technique, consisting of 5 steps from preprocessing, separation of RBCs from other blood components, discrimination between single RBCs and connected RBCs, segmentation of connected RBCs to final RBC counting, has been proposed. Results attaining a high accuracy have been demonstrated. The proposed minimum distance to

displacement ratio maximization criterion is intuitive and very promising for segmenting connected RBCs. Furthermore, by exploiting the geometry of convex objects, the proposed segmentation method is simple and effective for segmenting not only connected RBCs but also all other convex objects.

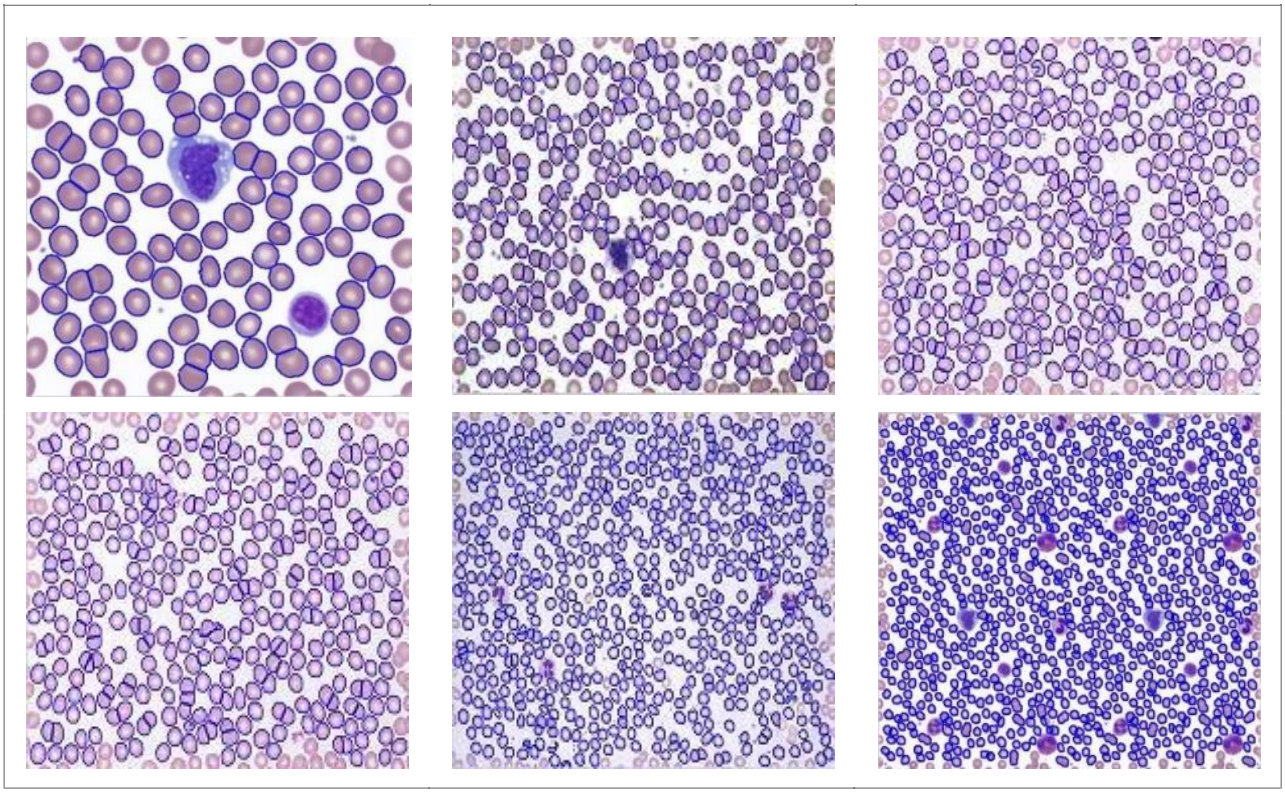

**Figure 8:** *Result images*

## REFERENCES

N Kanitsap, (2010) Iron status and prevalence of iron deficiency anemia in the elderly. Official Journal of the Thai Society of Hematology and the National Blood Centre The Thai Red Cross Society, 20, 287-296.

S Kareem, R.C.S Morling, I Kale (2011). A novel method to count the red blood cells in thin blood films, IEEE International Symposium Circuits and Systems, 1021- 1024. doi: 10.1109/ISCAS.2011.5937742

Pradipta Maji, Ankita Mandal, Madhura Ganguly, Sanjoy Saha. (2015) an automated method for

counting and characterizing red blood cells using mathematical morphology. International conference Advances in Pattern Recognition, 1-6. Doi: 10.1109/ICAPR.2015.7050674

Sumeet, G Rani. (2014). Automatic red blood cell counting using watershed segmentation. International Journal of Computer Science and Information Technologies, 5(4), 4834-483.

Siti Madihah Mazalan, Nasrul Humaimi Mahmood, Mohd Azhar Abdul Razak. (2013). Automated red blood cells counting in peripheral blood smear image using circular hough transform. International Conference on Artificial Intelligence, Modeling & Simulation, 320-324. Doi: 10.1109/AIMS.2013.59

Heidi Berge, Dale Taylor, Sriram Krishnan, Tania S. Douglas. (2011). Improved red blood cell counting in thin blood smear. IEEE International Symposium on Biomedical Imaging: From Nano to Macro, 204 – 207. Doi: 10.1109/ISBI.2011.5872388

Lorenzo Putzu, Cecilia Di Ruberto. (2013). White blood cells identification and counting from microscopic blood image. International Journal of Medical, Health, Biomedical and Pharmaceutical Engineering, 7(1), 189-196. Doi: scholar.waset.org/1999.9/189

Nasrul Humaimi Mahmood, Poon Che Lim, Siti Madihah Mazalan, Mohd Azhar Abdul Razak. (2013). Blood cells extraction using color based segmentation technique. International Journal of Medical, Health, Biomedical and Pharmaceutical Engineering. 7(1). doi: 10.1.1.300.3596

Nasution, A.M.T., EK Suryaningtyas. (2008). Comparison of red blood cells counting using two algorithms: connected component labeling and back projection of artificial neural network. IEEE Photonics Global Singapore, 1–4. Doi: 10.1109/IPGC.2008.4781402

Wilhelm Burger, Mark J. Burge. (2011). Digital image processing: an algorithmic introduction using java, Springer, 223-226.

Matt Sottile. (2013, January 11). Finding dents in a blobby shape. Mjsottile computational science and languages. Retrieved from http://syntacticsalt.com/2013/01/11/finding-dents- in-an-blobby-shape